DEUTSCHES ELEKTRONEN-SYNCHROTRON DESY
DESY SR 87-02
March 1987

STRUCTURE DETERMINATION OF ADSORBATES ON SINGLE CRYSTAL ELECTRODES WITH X-RAY STANDING WAVES

by

G. Materlik

Hamburger Synchrotronstrahlungslabor HASYLAB at DESY

M. Schmäh, J. Zegenhagen

II. Institut f. Experimentalphysik, Universität Hamburg

W. Uelhoff

Institut für Festkörperforschung, KFA Jülich

ISSN 0723-7979

NOTKESTRASSE 85 · 2 HAMBURG 52

To be sure that your preprints are promptly included in the
HIGH ENERGY PHYSICS INDEX ,
send them to the following address (if possible by air mail) :

DESY
Bibliothek
Notkestrasse 85
2 Hamburg 52
Germany

DESY SR 87-02
March 1987

ISSN 0723-7979

Structure Determination of Adsorbates on Single Crystal Electrodes with X-Ray Standing Waves

G. Materlik

Hamburger Synchrotronstrahlungslabor HASYLAB at DESY,

Notkestr. 85, D-2000 Hamburg 52

M. Schmäh and J. Zegenhagen

II. Institut für Experimentalphysik, Universität Hamburg,

Luruper Chaussee 149, D-2000 Hamburg 50

and W. Uelhoff

Institut für Festkörperforschung

der KFA Jülich GmbH, Postfach 1913, D-5170 Jülich

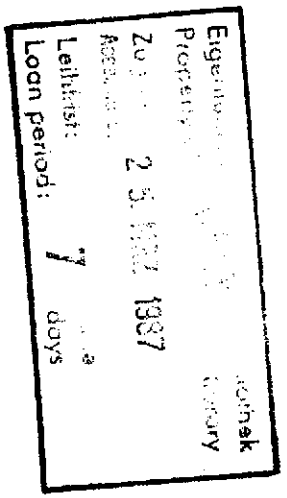

Abstract

Tl submonolayers were deposited from an aqueous electrolyte on a Cu(111) surface. The electrodes were studied inside and outside the electrolyte with standing x-ray wave fields. These measurements allow to determine the fraction and the position of Tl atoms which occupy adsorption sites coherently relative to the bulk diffraction planes. The results show that the method can be applied to ex-situ as well as in-situ structure studies of the solid/liquid interface. The influence of oxygen on immersed and emersed Cu electrodes is discussed in detail.

---

to be published in Ber. Bunsenges.

Introduction

The determination of the atomic structure of an electrochemical interface poses an almost unsurmountable problem to methods such as electron scattering (LEED, RHEED, etc.), ion scattering, and scanning tunneling microscopy. The high sensitivity of particle probes, which make them on one hand an ideal tool for studies of surfaces, becomes a strong drawback if such surfaces are covered by a solid or liquid layer. Such a thin cover of the interface, however, is transparent for high energy x-ray photons which exhibit a comparatively low interaction with matter. Strong photon sources are therefore needed to gain a large enough signal from the interface atoms in order to be able to carry out a structure determination. Sources of sufficent brilliance are nowadays available as electron/positron storage rings which emit highly intense synchrotron radiation.

In addition to the powerful source a proper experimental method has to be designed to determine the geometric structure of the atomic arrangement in the interface. One possibility is to use coherent x-ray interference fields, described by the dynamical theory of x-ray diffraction [1,2]. Such x-ray standing waves (XSW) were used for the first time in 1980 [3] to determine the distance of a chemisorbed Br layer normal to a Si(110) surface. The application for the study of emersed Cu electrodes was reported in 1985 [4] and the first in-situ investigation has meanwhile also been finished successfully [5]. A brief review of the most recent applications of XSW using synchrotron radiation is given in [6].

The principle of the method for in-situ studies of electrodes is illustrated in Fig. 1. A nearly plane wave like x-ray beam ($\underline{E}_o^o \exp(2\pi i \underline{K}_o \cdot \underline{r} - i\omega t)$ impinges through the liquid electrolyte layer onto a $\underline{H}$ = (111) oriented surface of a perfect Cu single crystal, $\underline{H}$ being the

reciprocal lattice vector. When the angle θ between the incident wave vector $\underline{K}_O$ and the diffraction planes is tuned to fulfill the Laue condition $\underline{K}_O + \underline{H} = \underline{K}_H$, a strong Bragg reflected beam $[\underline{E}_H(\underline{r},\theta,t) = \underline{E}_H^O \exp(2\pi i \underline{K}_H \cdot \underline{r} - i\omega t)]$ with wave vector $\underline{K}_H$ is excited. In the region where both waves are coexisting, an interference field is formed with nodal and antinodal planes lying parallel to the $\underline{H}$ diffraction planes and with the spatial periodicity $d_H = 1/|\underline{H}|$. The antinodal planes of the electrical field intensity $|\underline{E}_{int}(\underline{r},\theta)|^2 = |\underline{E}_O(\underline{r},\theta) + \underline{E}_H(\underline{r},\theta)|^2$ move inward with increasing reflection angle θ in the $-\underline{H}$ direction from being out of phase with the H Fourier component of the elastically scattering electron density to being in phase with the diffraction planes.

Since the photoeffect for inner core electrons is, in the dipole approximation, proportional to the E-field intensity at the center of the atom, this movement of the standing-wave field can be used to determine atomic positions relative to the diffraction planes by measuring simultaneously with the wave field shift, emission signals such as fluorescence photons which can also penetrate the liquid layer. Fig. 2 shows reflectivity $[|\underline{E}_H|^2/|\underline{E}_O|^2]$ and fluorescence yield data and theoretical fits from an XSW measurement on a Cu(111) single crystal, which was removed at a fixed potential from an aqueous Na_2SO_4 solution after deposition of a Cd layer. The Cu L emission originates from the topmost about 150 Å thick region of the substrate. Cd was intentionally deposited via the potential control. Sulfur originates from the Na_2SO_4 and Cl from the calomel reference electrode. The fluorescence measurement with an energy dispersive Si(Li) solid state detector reveals this coexistence of different atomic species simultaneously and the chemical as well as structural composition can be determined. From the different shapes of the Cd, Cl, S and Cu fluorescence yield curves in Fig. 2 it is obvious that they are coexisting in different adsorption geometries. While the Cu occupies as expected

substitutional sites, the Cl atoms are incoherently distributed and Cd, S show coherent adsorption which can be evaluated in detail. However, this attempt goes beyond the scope of this article.

Experiment

The XSW measurements were done at the ROEMO station of the Hamburg Synchrotron Radiation Laboratory HASYLAB. The experimental arrangement is shown schematically in Fig. 3. Synchrotron radiation emitted from the storage ring DORIS was monochromatized by a double crystal arrangement [7,8] which consisted of a symmetric Ge(220)(X1) and an asymmetric Si(220)(X2) crystal. This combination of crystals allowed the proper photon energy to be selected (15.3 keV for the ex-situ and 12.8 keV for the in-situ study). In addition, the use of an asymmetric Si crystal reduced the monochromator angular emittance to about one tenth of the Cu(111) reflection curve, thereby better approximating the plane wave case for the beam incident on the sample crystal. The ion chambers were used to keep the monochromator aligned (I1), and to monitor (I2) the flux incident on the sample (XS). The ex-situ situation is shown as sample environment in Fig. 3. For the in-situ study, a specially developed thin film cell (see below) was used to maintain a liquid film of constant thickness at controlled potential conditions.

Collimators were used to reduce the radiation background (S1, S2) and to choose a proper sample area (S3). The NaI (Tl) detector measured the Cu reflectivity as a function of sample reflection angle θ (ex-situ) or incident wavelength λ (in-situ). In the latter case, both monochromator crystals were rocked simultaneously to change the wavelength. As discussed for the case of ultrahigh vacuum XSW studies, the energy dispersive mode has to be used if sample environments require that the sample cannot be

rocked throughout a measurement. The Si(Li) solid state detector recorded the scattered photons at 16 or 32 different angular/wavelength settings. An aluminium absorber (A) of properly chosen thickness in front of the Si(Li) avoided overloading of the detector system from the strong Cu K substrate fluorescence. The XSW instrument is described in detail elsewhere [4,8-10].

Analysis

The analysis of XSW measurements has been discussed in detail in [4,7,11] and we will here only give a qualitative description as far as it is needed to understand the implications of the two parameters which are determined from an XSW analysis: the coherent fraction $f_{c,H}$ and the position Φ_H which are the amplitude and the phase of the H Fourier component of the adsorbate density distribution function, respectively. Fig. 4a) shows adsorbed atoms which only occupy one position $d_{Ads} = \Phi_H d_H$, and Φ_H gives therefore the atomic position in the direction $\underline{H}$ in units of the bulk diffraction plane spacing d_H. If all adsorbate atoms occupy just one position, $f_{c,H} = 1$. Fig. 4b) depicts a case in which two positions are occupied. At each position of the H standing wave only a fraction of atoms will be in phase with the wave field. The results will then be $f_{c,H} < 1$ and a weighted average value for Φ_H. As also indicated in Fig. 4b, the choice of a different diffraction plane $\underline{H}^*$ will change this situation and give additional information to fully describe this distribution function.

For the present study we have carried out measurements of Tl on Cu(111) with $\underline{H}$ = (111). For the analysis we have assumed a Tl distribution model in which f_c Tl atoms occupy sites Φ_{111} as determined from the measured Tl L fluorescence yield and the Cu(111) reflectivity, and $(1-f_c)$ atoms are distributed randomly in the direction $\underline{H}$.

Ex-situ Study

XSW measurements on Cu electrodes which were removed from the electrolyte are in length discussed in ref. 4. The underpotential deposition of metal ions was performed in an electrochemical cell (insert in Fig. 5) with a Pt counterelectrode (C), a saturated calomel electrode (SCE) as reference electrode (R), and with the Cu electrode (X) dipping into the 0.5 M Na_2SO_4 and 10^{-3} M $TlNO_3$ electrolyte. The potential was controlled by a potentiostat (Pot.) and the current potential curve was recorded with an X-Y recorder (Rec). Current potential curves which are characteristic for two different kinds of preparations are shown in Fig. 5. Curve (a) was recorded with nitrogen flowing through the electrolyte to reduce the oxygen partial pressure. In this case the N_2 left the electrochemical cell through a small open hole in the cover. Curve (b) was recorded when the gas outlet was closed such that N_2 was flowing at the outlet through a vapour lock to prevent any oxygen from diffusing back into the electrochemical cell. The influence of oxygen in the solution is clearly visible in the current potential curve (b). After the scan was stopped, the electrode was removed from the solution and the electrolyte was carefully peeled off the surface before the XSW measurement was done under normal atmospheric conditions. Fig. 6a) shows for several different preparations the measured position d_{111}^{Tl} of the Tl atoms as a function of coverage Θ_{Tl} and part b) shows the corresponding coherent fraction f_c^{Tl}. Since the phase value Φ_{Tl} is determined in units of the bulk diffraction plane spacing, the d_{111}^{Tl} value gives the Tl distance from the topmost Cu diffraction plane.

The decrease of f_c^{Tl} with increasing Θ_{Tl} can be explained by adsorption of Tl at disordered parts of the Cu substrate surface. An increase of surface roughness from electrochemical polishing has also been observed with electron microscopy [12]. Rinsing the sample with water right after

the removal from the electrolyte increased f_c^{Tl} (full circles and full rectangles in Fig. 6) because the additional incoherently adsorbed Tl was flushed off. A coherent adsorption at other sites can be excluded from our measurement, because the position d_{111}^{Tl} (Fig. 6a) does not show a significant dependence on Θ_{Tl}.

Clearly visible in part a), however, are two different groups of results for adsorption in an electrolyte with and without oxygen. Averaging over preparations with and without oxygen gives for $\langle d_{111}^{Tl} \rangle$ results of (2.27 ± 0.04)Å and (2.67 ± 0.02)Å, respectively.

In Situ-Study

Since perfect Cu crystals are very sensitive to mechanical strains, a special electrochemical cell, seen in Fig. 7, had to be constructed for XSW measurements on Cu single crystals covered with a thin liquid electrolyte film. This cell replaced the sample shown in Fig. 3. The body of the cell was made from PTFE and a 4 µm thick Mylar foil was used as window for the x-ray photons. This foil limited the layer thickness on one side and kept by capillary action the fluid from running down between the Cu crystal and the softly sealing Teflon lips. The thickness of the layer can be adjusted form about 20 to 50 µm by carefully pumping on the electrolyte. The pump also serves for exchange of the electrolyte and to establish a contact to the reference and counter electrodes. Therefore, a Tl layer of about 1 ML can be deposited on the Cu surface and the electrolyte can be cleaned from surplus Tl after that by exchange with pure 0.5 M Na_2SO_4 solution. The Tl concentration was chosen such that it contanied about 10^{15} Tl ions/cm^2 within the thin layer ontop of the Cu crystal. The whole cell, tubing and electrolyte reservoirs were placed inside a containment filled with nitrogen because of the high sensitivity of the electrochemical process to

oxygen. Fig. 8 shows two current potential curves typical for electrolytes with (a) and without oxygen (b) influence. As in the ex-situ case (Fig. 5) a clear difference is visible.

The difference between corresponding curves in Figs. 5 and 8 is mostly caused by the different Tl concentrations which are present during the sweep. For the in-situ measurement, the surplus Tl in the outer layer between the Cu and the window has to be removed to lower the fluorescence background from Tl ions in the solution such that the signal from the adsorbed Tl layer can be clearly discriminated. Therefore, the cycle time for the diagrams in Fig. 8 is too short to enable bulk deposition of the Tl in the solution.

The XSW results from two measurements at constant potential (top curve: -0.71 V vs SCE; bottom curve: -1.00 V vs SCE) are shown in Fig. 9. Already the comparison of the shape of the fluorescence curves displays a difference in adsorption geometry. The detailed analysis showed that results for d_{111}^{Tl} ranged from (2.28 ± 0.1)Å on the small distance side to (2.64 ± 0.05)Å on the large distance side. Derivation of a mean value $\langle d_{111}^{Tl} \rangle$ for preparations without oxygen give (2.58 ± 0.02)Å which has to be compared with the corresponding ex-situ value (2.67 ± 0.02)Å.

No significant dependence of the measured adsorption site on the applied potential was found, but other measured distances between the above limits are characteristic of mixtures of surface areas where Tl is directly adsorbed to the Cu atom and others in which the Cu surface layer has been changed by the presence of oxygen prior to Tl adsorption. As discussed in detail for the ex-situ case [4] the smaller distance of the Tl relative to the topmost Cu diffraction plane can be explained by the incorporation of oxygen into the Cu topmost surface layer.

Discussion

The difference of 0.09 Å between the mean values $\langle d_{111}^{Tl} \rangle$ of the ex-situ and in-situ measurements of the clean surface can be a hint towards an effect on the adsorbate caused by the sudden potential change upon extraction of the crystal from the solution. It can be ruled out from the potential current curves, that the solution contained in all in-situ cases more oxygen than the corresponding electrolyte used for the ex-situ measurement. While the ex-situ value is consistent with a model in which Tl adsorption takes place at two-fold sites together with a contraction of the Tl radius (1.73 Å) by 3%, the in-situ value (2.58 ± 0.02)Å can be explained by adsorption at three-fold sites coupled with a 3% Tl contraction. Adsorption at the one-fold site can be excluded in both cases.

The effect of oxygen on the position of the topmost Cu layer is controversal. An inward shift of the Cu layer by about 0.3 Å was deduced from ion scattering data [13]. Theoretical calculations for O on Ni [14] indicate that O is built in below the top layer, thereby pushing the Cu atoms out of the surface and opening a larger three-fold hole for the Tl atom binding, taking place at a reduced distance as shown in Fig. 10. A detailed discussion of this model and a comparison to semiempirical values for the O-Cu bondlength at the surface [15] is given elsewhere [5].

Summary

It has been demonstrated that the structure of the solid/electrolyte interface can be studied successfully with x-ray standing-wave fields. The first comparison of ex-situ and in-situ measurements of the Tl adsorption on Cu(111) has given new results on this system under normal atmospheric conditions as well as in the electrolyte. Further Fourier components of the

Tl density distribution function are needed to fully characterize the structure also in the lateral in-plane arrangement.

Acknowledgement

We like to thank Prof. D.M. Kolb for many discussions and valuable advice on electrochemistry as well as for the loan of electrochemical equipment, and A. Fattah for his skillful help in preparing the Cu crystals. The project is supported by the German Federal Minister for Science and Technology.

Figure Captions

Figure 1

Schematic of the solid/electrolyte interface with x-ray beam path and standing-wave field.

Figure 2

Measured and calculated reflectivity (□, ...) and Cu-L fluorescence yield (■, -) of a (111) Cu crystal together with fluorescence yields of simultaneously measured co-adsorbed Cl (Δ, ---), S (●, -•-) and Cd (○, --) atoms.

Figure 3

Experimental XSW set-up (for details see text).

Figure 4

Illustration of XSW measurement with reflections H, H* and one position (a) and two position (b) adsorbate density distributions.

Figure 5

Current-potential curves for Cu(111) in 0.5 M Na_2SO_4 + 1 mM $TlNO_3$, containing a trace amount of oxygen (a) and without oxygen contamination (b). The inset shows the electrochemical set-up (see text). Immersed Cu surface areas: (a) 1.13 cm^2, (b) 0.8 cm^2. Potential sweep rate: (a) 200 mV s^{-1}, (b) 100 mV s^{-1}.

Figure 6

Position (a) and coherent fraction (b) results from several XSW measurements (different symbols) as function of total Tl coverage Θ_{Tl}. ◇ and ◈ are from measurements without oxygen present in the electrolyte.

Figure 7

Thin film cell for in-situ studies.

Figure 8

Current-potential curves for Cu(111) recorded in the in-situ cell with an electrolyte containing a trace amount of oxygen (a) and without oxygen contamination (b).

Figure 9

Measured and calculated reflectivity (+, ---) and fluorescence yield curves from in-situ measurements with oxygen (⊕, -) and without oxygen (⊕, -•-).

Figure 10

Model for Tl adsorption on a Cu(111) surface with incorporated oxygen. Δd_R is the outward Cu relaxation caused by the embedded O.

References

1 M. v. Laue, **Röntgenstrahlinterferenzen** (Akademische Verlagsgesellschaft, Frankfurt/Main, 1960)

2 Z.G. Pinsker, **"Dynamical Scattering of X-Rays in Crystals"** (Springer Verlag, Berlin 1978)

3 P.L. Cowan, J.A. Golovchenko, and M.F. Robbins, Phys. Rev. Lett. **44**, 1680 (1980)

4 G. Materlik, J. Zegenhagen, and W. Uelhoff, Phys. Rev. **B32**, 5502 (1985); J. Zegenhagen, G. Materlik, W. Uelhoff (in preparation)

5 G. Materlik, M. Schmäh and W. Uelhoff (to be published)

6 G. Materlik, Z. Physik B - Condensed Matter **61**, 405 (1985)

7 G. Materlik and J. Zegenhagen, Phys. Lett. **104A**, 47 (1984)

8 A. Krolzig, G. Materlik, M. Swars, and J. Zegenhagen, Nucl. Instrum. Methods **219**, 430 (1984)

9 P. Funke and G. Materlik, Sol. Stat. Comm. **54**, 921 (1985); P. Funke, G. Materlik, and A. Reimann, Nucl. Instrum. Methods **A246**, 763 (1986)

10 A. Krolzig, G. Materlik, and J. Zegenhagen, Nucl. Instrum. Methods **208**, 613 (1983)

11 N. Hertel, G. Materlik, and J. Zegenhagen, Z. Phys. **58**, 199 (1985)

12 Y. Uchida, G. Lehmpfuhl, and J. Jäger, Ultramicroscopy **15**, 119 (1984)

13 H. Niehus, Surf. Sci. **130**, 41 (1983)

14 B. Chakrabolty, S. Holloway, and J.K. Norskov, NORDITA preprint 84/7

15 K.A.R. Mitchell, Surf. Sci. **155**, 93 (1985)

FIG. 1

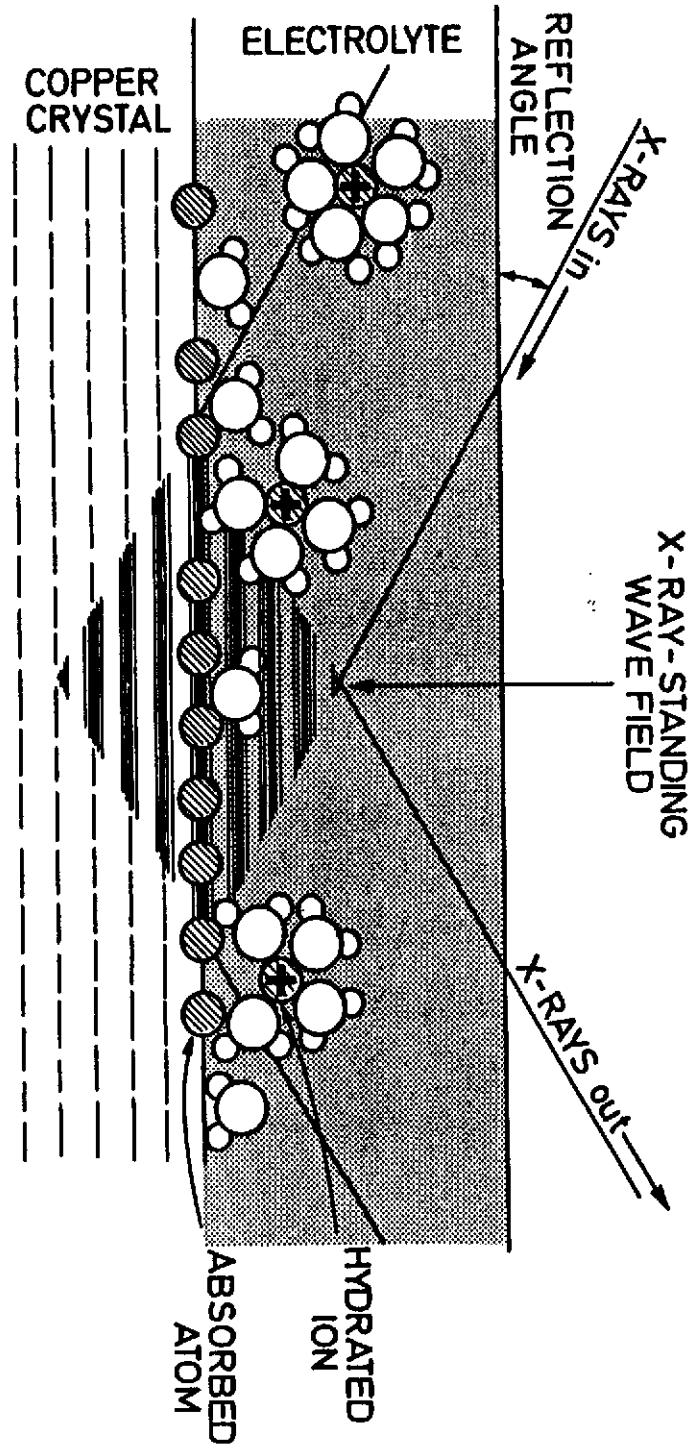

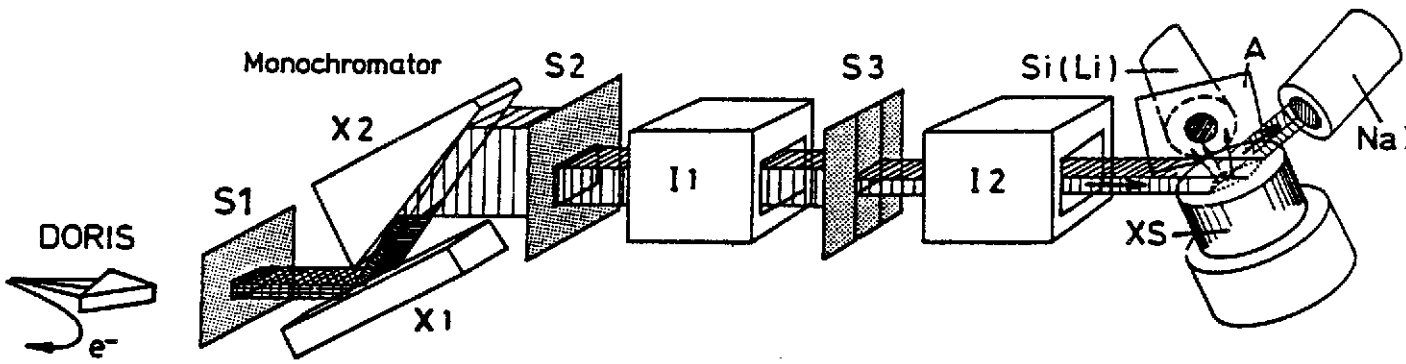
Monochromator
S2
S3
Si(Li)
A
X2
S1
I1
I2
NaI
DORIS
XS
X1
e⁻

FIG. 3

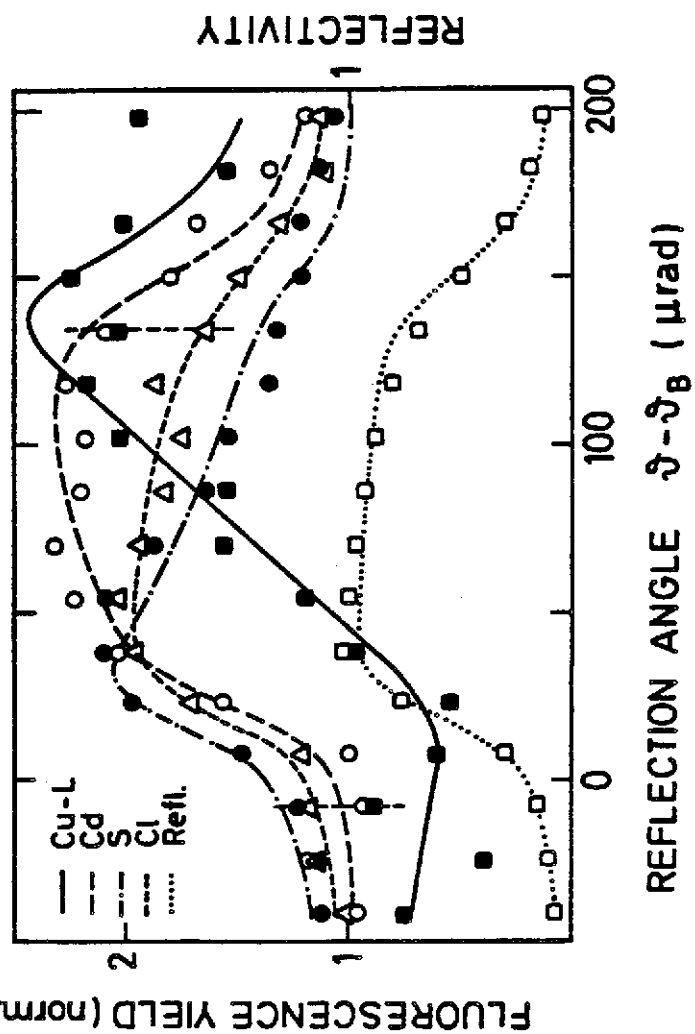
REFLECTIVITY
FLUORESCENCE YIELD (norm.)
REFLECTION ANGLE ϑ-ϑB (μrad)
Cu-L
Cd
Sn
Cl
Refl.
1
2
0
100
200

FIG. 2

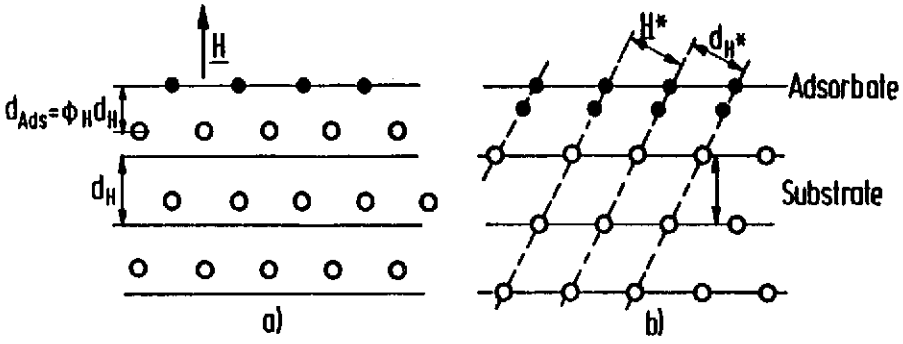
H
$d_{Ads}=\Phi_H d_H$
d_H
a)
H*
d_H*
Adsorbate
Substrate
b)

FIG. 4

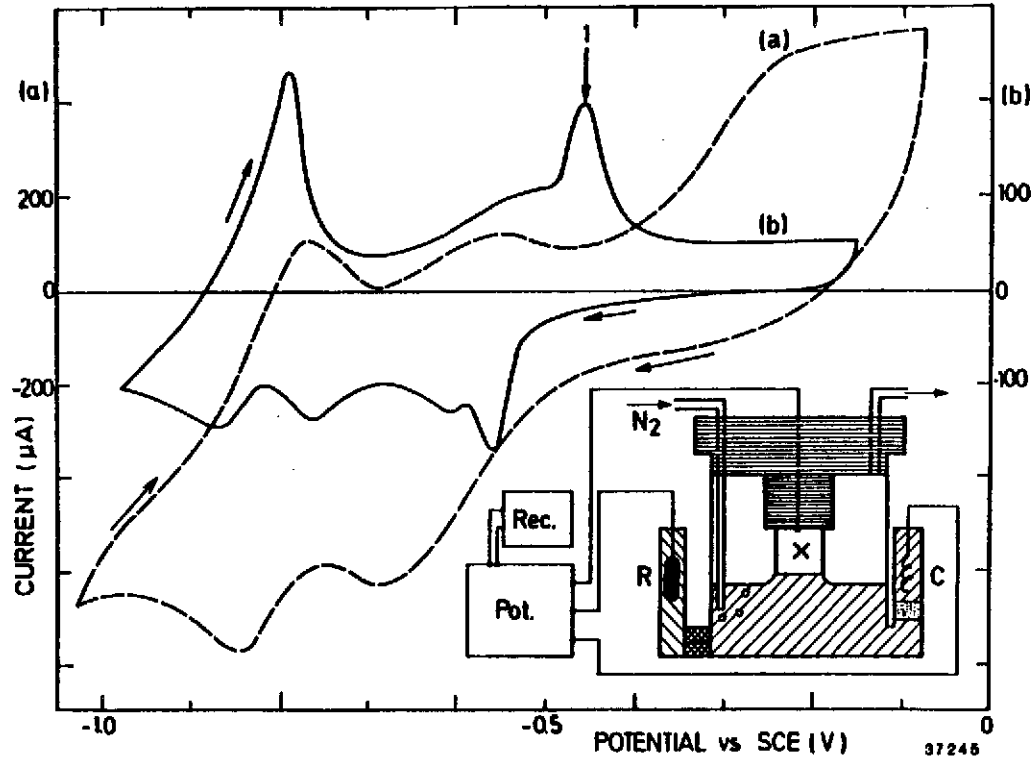
(a)
(b)
1
200
0
-200
CURRENT (μA)
-1.0
-0.5
0
POTENTIAL vs SCE (V)
100
-100
N_2
Rec.
Pot.
R
C
37245

FIG. 5

FIG. 6

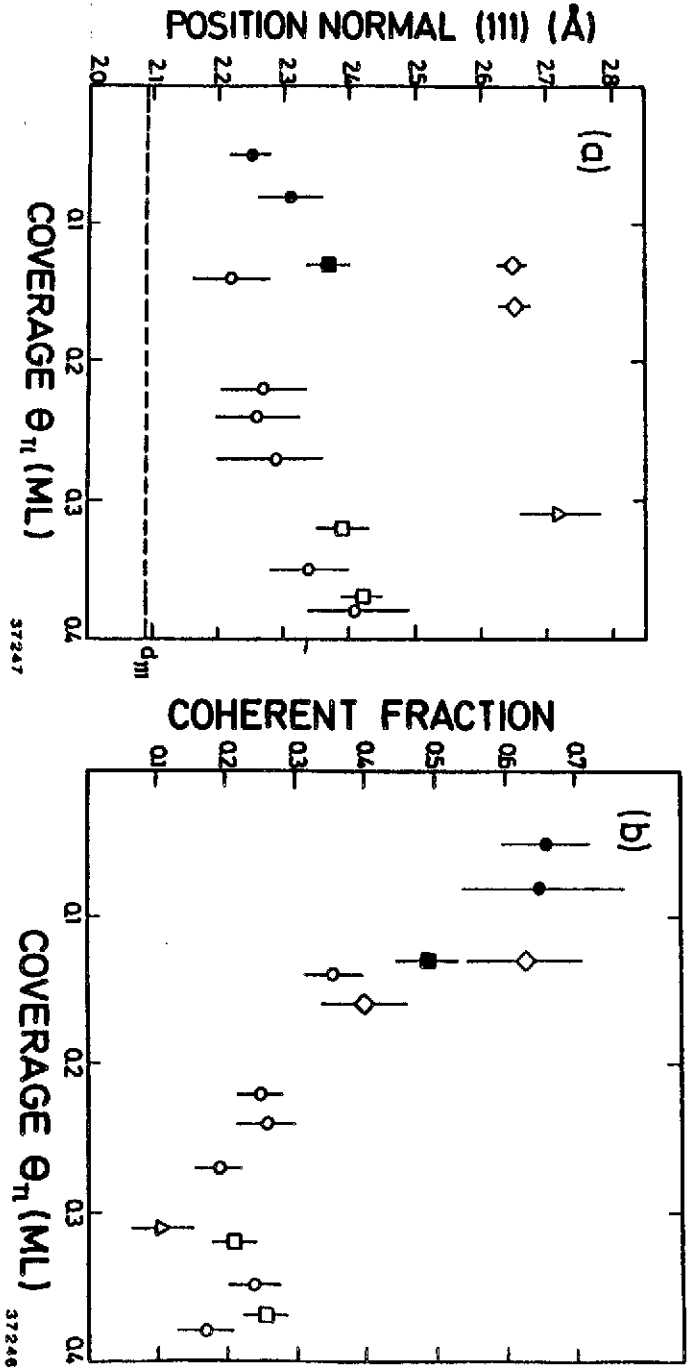
POSITION NORMAL (111) (Å)
2.0
2.1
2.2
2.3
2.4
2.5
2.6
2.7
2.8
(a)
COVERAGE Θ_{Tl} (ML)
0.1
0.2
0.3
0.4
d_{111}
37247
COHERENT FRACTION
0.1
0.2
0.3
0.4
0.5
0.6
0.7
(b)
COVERAGE Θ_{Tl} (ML)
0.1
0.2
0.3
0.4
37248

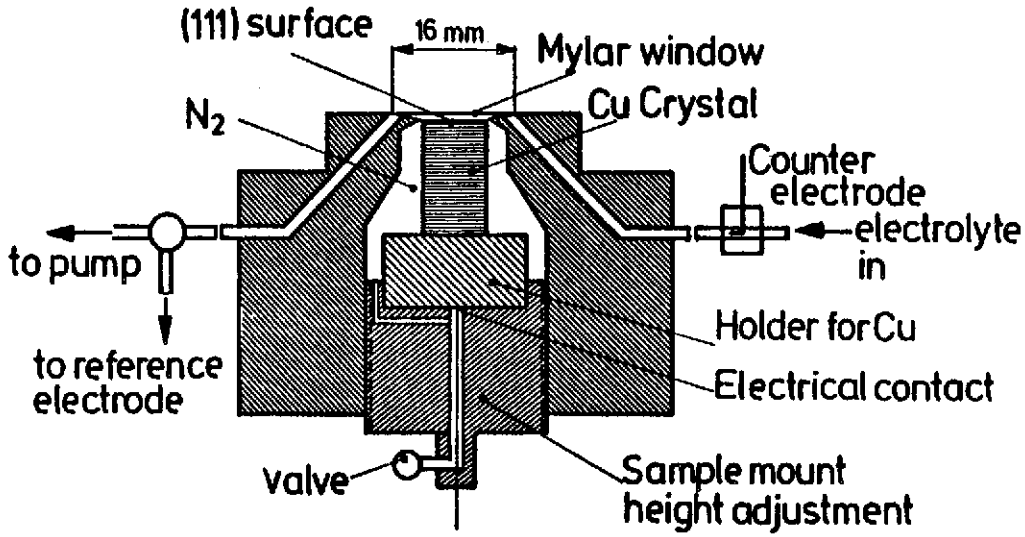
(111) surface
16 mm
Mylar window
Cu Crystal
N_2
Counter electrode
electrolyte in
to pump
to reference electrode
Holder for Cu
Electrical contact
valve
Sample mount height adjustment

FIG. 7

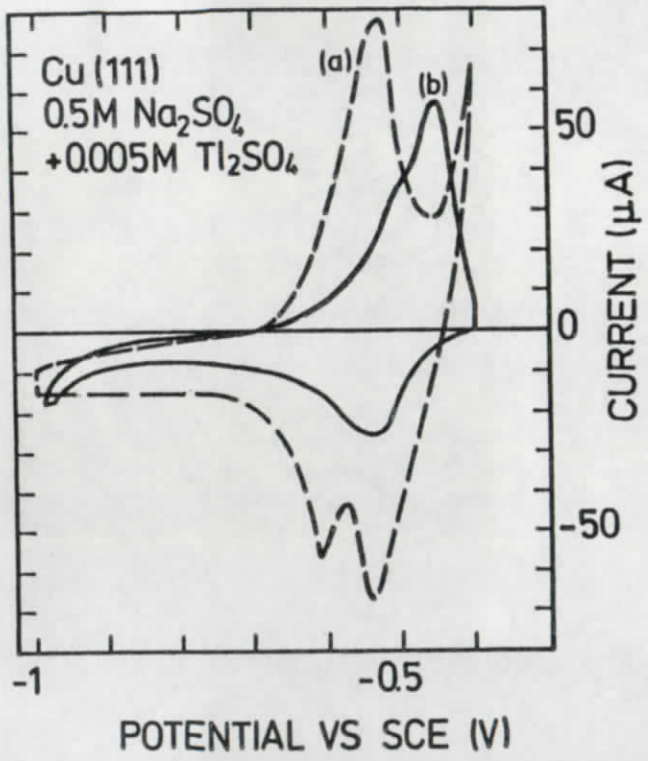
Cu (111)
0.5M Na_2SO_4
+0.005M Tl_2SO_4
(a)
(b)
50
0
-50
CURRENT (μA)
-1
-0.5
POTENTIAL VS SCE (V)

FIG. 8

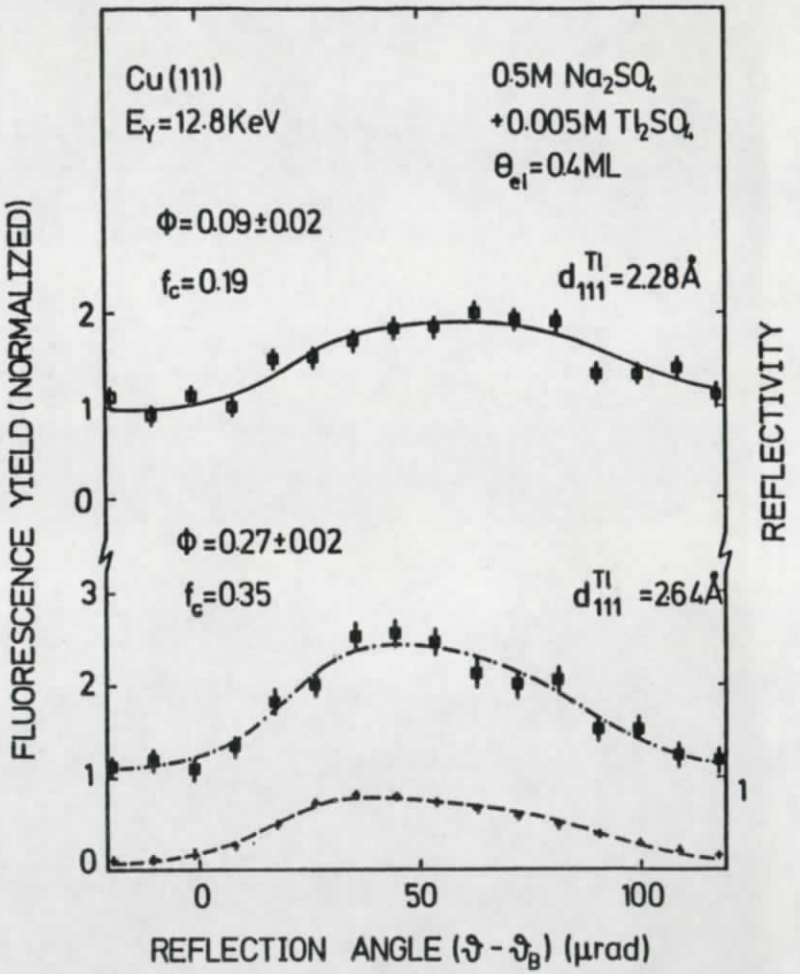
Cu (111)
E_γ=12.8KeV
0.5M Na_2SO_4
+0.005M Tl_2SO_4
θ_{el}=0.4ML
Φ=0.09±0.02
f_c=0.19
d_{111}^{Tl}=2.28Å
Φ=0.27±0.02
f_c=0.35
d_{111}^{Tl}=2.64Å
FLUORESCENCE YIELD (NORMALIZED)
REFLECTIVITY
0
50
100
REFLECTION ANGLE ($\vartheta - \vartheta_B$) (μrad)

FIG. 9

SIDE VIEW ALONG [0$\bar{1}$1]

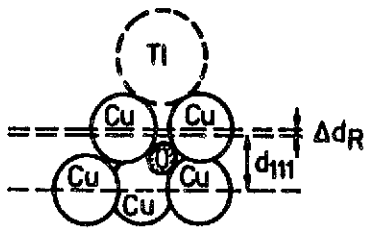

TOP VIEW ALONG [111]

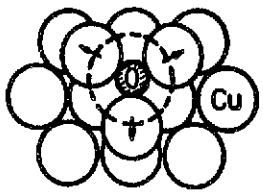

FIG. 10